Radial density distribution of the metastable supersaturated vapor via restricted ensemble simulations

Chu Nie[1,*] and W. H. Marlow[2]
[1]*School of Physics and Information Engineering, Jianghan University, Wuhan, 430056, People's Republic of China*
[2]*Department of Nuclear Engineering, Texas A&M University, College Station, Texas 77843, USA*
(Received 3 March 2008; published 16 July 2008)

Extensive restricted canonical ensemble Monte Carlo simulations [D. S. Corti and P. Debenedetti, Chem. Eng. Sci. **49**, 2717 (1994)] for the supersaturated Lennard—Jones (LJ) vapor were performed. These simulations were conducted at different densities and reduced temperatures from 0.7 to 1.0 and the radial density distribution functions were obtained, most of which are unavailable via integral equation theory due to phase separations. Among different constraints imposed on the system studied, the one with the local minimum of the excess free energy was taken to be the one that approximates the equilibrium state of the metastable LJ vapor. For the slightly saturated state points, where integral equation theory does have a solution, compared with our simulations, differences of the radial density distribution functions were found and they are attributed to ignoring density fluctuations in the integral equation theory.

DOI: 10.1103/PhysRevE.78.012101 PACS number(s): 64.60.My, 61.20.Ja

I. INTRODUCTION

The thermal properties of the supersaturated vapor are interesting and important because of their scientific and engineering applications. Numerous research works have contributed to this field with their special interests [1–19]. For example, some focus on the free-energy barrier of the nucleus, the critical size of the liquidlike drop, or homogeneous condensation of the supersaturated vapor [1–13]; other studies deal with the thermal properties of the supersaturated vapor itself [14–18]; and others discuss the failure of the integral equation with various approximations when applied to a metastable system [19,20].

Without a doubt, the integral equation theory provides a method of relatively low computational cost to investigate the thermal properties of both simple and complex fluids. The radial density distribution function $g(r)$ can be easily obtained and numerous thermal properties can be obtained from $g(r)$, for example the internal energy, pressure or even chemical potential, and so on. Although great successes have been achieved, when applied to the metastable fluid, the integral equation method has been found to have some unsolvable regions for certain densities and temperatures [19–22]. The unsolvability of the integral equation was found to result from the presence of square root branch points that signal the onset of complex solutions [23]. Efforts have been made to seek the solution inside the unsolvable region, for example those listed in Refs. [20,23], and many solutions were found [22]. Therefore, so far, except for very slightly saturated cases, most of the state points inside the spinodal cannot be solved with the integral equation.

Corti and Debenedetti [16] emphasized that the difference of equilibrium between the normal state and the metastable state lies in the number of configurations appearing in the two kinds of systems. For a normal state, the probability of the appearance of a state is governed by the Boltzmann factor, and the higher the system energy is, the lower is the probability that it will appear. However, in the metastable system, there exists an energy barrier. Once the system overcomes the barrier, the system goes to phase separation. Therefore, the central task for the simulation is to prevent the system from going to phase separation.

Recalling the derivation of the integral equation [24,25], the integral equation is derived from the Mayer cluster expansion [26], and the various approximate closure relationships were obtained by manipulating or ignoring some diagams in the expansion. Thus all integrations in the partition function are performed without considering the density fluctuation of the atoms or molecules in configuration space, which appeared to be vital when dealing with the metastable fluid [16–18]. Also, as explicitly pointed out in Ref. [27], in order to obtain the thermal properties of the metastable fluid, a constraint potential must be added to the partition function, which apparently alters the partition function. Linhart *et al.* [17] developed a molecular-dynamics (MD) simulation method to study the thermal properties of the supersaturated vapor up to spinodal density at different temperatures. They averaged the thermal properties before the system goes to phase separation and used the instantaneous pressure, the numbers of atoms in the largest cluster, and the number of atoms not belonging to any cluster to indicate phase separation. Recently, we reported the pressure, excess chemical potential, and excess free energy, with respect to ideal-gas data at different densities of the supersaturated Lennard-Jones (LJ) vapor at the reduced temperature 0.7 by use of the restricted canonical ensemble Monte Carlo simulation method [18]. At each density studied, we imposed different constraints on the system and found for those densities below the spinodal density that the system would exhibit a free-energy local minimum, which is close to the equilibrium state of the metastable system. While the integral equation theory includes the integration of the phase-separated configurations, the radial density distributions obtained from such a theory will not be accurate, thus leading to the incorrect thermal properties of the metastable system. In this pa-

*niechu@hotmail.com

per, we will demonstrate these assertions by comparison with our simulation results.

II. METHODS AND SIMULATIONS

Here, we recapitulate the methodology we used previously [18]. In this work, the vapor is modeled by simulations with Lennard-Jones model interactions for atoms,

$$u(r) = 4\varepsilon\left[\left(\frac{\sigma}{r}\right)^{12} - \left(\frac{\sigma}{r}\right)^{6}\right]. \tag{2.1}$$

First, divide the system into subcells based on the number of atoms and the density of the system studied. The length of the cubic subcell is taken with the following relations:

$$l = \frac{L}{N^{(1/3)}}, \tag{2.2}$$

where L is the length of an edge of the simulation box and N is the total number of particles during simulation. Therefore, the ideal homogeneous case should correspond to one atom per cell. However, density fluctuations exist, and limiting the maximum number, i, of atoms in each subcell d_i may help to maintain the one phase state for the system studied. For a given density, a series run starts from $d_{\max}$, when no number limitation is imposed onto the subcell, to d_2, when only two atoms in one subcell are allowed; otherwise, the trial movement of a selected atom will be rejected. For each run, the excess chemical potential and pressure are averaged and recorded. With the obtained excess chemical potential and pressure, the excess free energy can be computed with the following formula:

$$f^{\mathrm{ex}} = \mu^{\mathrm{ex}} - P^{\mathrm{ex}}/\rho, \tag{2.3}$$

where f^{ex} is the excess free energy per particle, μ^{ex} is the excess chemical potential, and P^{ex} is the excess pressure of the system with respect to the ideal case, ρ^{id}. In this work, initially, all the atoms were placed on a simple cubic lattice. For all simulations, the system size was set at least to 40σ. The number of steps to reach equilibrium is 10×10^6 moves, and another 200×10^6 moves were used to sample the phase space. The cutoff distance is set to be 8.0σ, and beyond the cutoff distance, standard long-range corrections were employed. The simulations are carried out at $T^*=0.7$, 0.75, 0.8, 0.9, and 1.0, where $T^*=kT/\varepsilon$. For $T^*=0.7$, 0.75, and 0.8, the number of particles involved in the simulation is 3375, and for $T^*=0.9$ and 1.0, the number of particles involved in the simulation is 5832 and 6859, respectively. The excess chemical potential is measured by performing the brute force sampling of $\exp(-\beta u)$, where it is the energy increase brought by the insertion of a test atom. To see the original idea of the atom insertion method, the reader should refer to Ref. [28], and our program is made based on the classical textbooks on molecular simulation [29,30]. For the integral equation,

$$\gamma(r) = h(r) - c(r) = \int \rho h(r')c(r-r')dr', \tag{2.4}$$

where $h(r)$ is the total correlation function, $c(r)$ is the direct correlation function, and $\gamma(r)$ is the indirect correlation function. The Percus-Yevick (PY) closure is used,

$$h(r) = \exp[-\beta u(r)][1+\gamma(r)] - 1. \tag{2.5}$$

Throughout our calculation, we set the grid spacing to be 0.005σ and the total number of the grid points is 4096. The method of solution of the integral equation follows that presented in Ref. [31].

TABLE I. Simulation results for the excess free energy [in the table, $f' = \mu^{\mathrm{ex}} - (P^{\mathrm{id}} + P^{\mathrm{ex}})/\rho$ is listed] and constraints imposed on the system of supersaturated vapor. The cutoff distance was $r_c = 8.0\sigma$ and the system size was $N=3375$.

$d_{\max}/\rho\sigma^3$	0.03	0.035	0.04
2	−0.9923	−1.0426	−1.0926
3	−1.0428	−1.1006	−1.1578
4	−1.0717	−1.1336	−1.1967
5	−1.0867	−1.1558	−1.2267
6	−1.0970	−1.1716	−1.2641
7	−1.1085	−1.1714	−1.2531
8	−1.0939	−1.2013	−1.2584
9	−1.0976	−1.1968	−1.3668
10	−1.1038	−1.2175	−1.3785
∞	−1.9477	−2.0068	−2.3899

III. RESULT AND DISCUSSION

First, we show an example of how to identify the approximated equilibrium state of the metastable fluid by locating the local minimum of free energy. Table I gives simulation results at three densities for the excess free energy per particle and constraints imposed on the supersaturated vapor system at $T^*=0.7$. These three examples correspond to the lightly saturated cases under the temperature studied. It is clearly seen in the table that for each column, the excess free energy per particle first increases, then decreases to a minimum value, then increases a bit, and finally decreases. Thus the local minimum free energy is clearly seen and located. For the last row ($d_{\max}=$inf) in the table, the free-energy values are much higher than the upper ones, which indicates that the simulations were performed under the circumstances of phase separations.

Second, we show two examples that even for the slightly saturated cases at different temperatures, the pressures predicted by the integral equation theory exhibit a systematic difference compared with the result obtained by the current simulation method. Figures 1 and 2 give the result of the radial density distributions for $\rho\sigma^3=0.06$ at $T^*=0.9$ and $\rho\sigma^3=0.08$ at $T^*=1.0$, respectively, where the integral equation method does have solutions. It is clearly seen that for the two cases studied, the first peak of the radial density distribution functions from the integral equation method are broader and higher than those obtained from the simulation method. Since it does not take the density fluctuations of the atoms into account, this indicates that for the integral equation method, the partition functions it manipulates involve

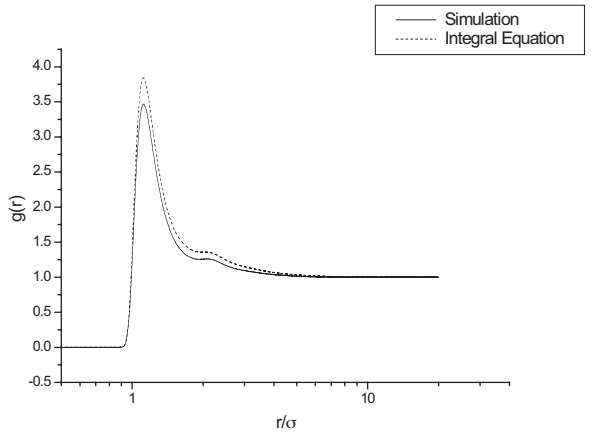

FIG. 1. Radial density distribution functions obtained from the simulation method for $\rho\sigma^3=0.06$ at $T^*=0.9$.

contributions from the phase-separated configurations. While not overwhelming as for the highly saturated cases, these contributions help to broaden and enlarge the first peak of the radial density distribution functions. It is the small part of the liquid phase, including in the integral equation theory, that contributes the higher first peak in both Figs. 1 and 2. For the simulation method applied in this work, the phase separation is effectively prevented by dividing the system studied into subcells and limiting the maximum number of atoms appearing in each subcell, which yields a lower and narrower first peak.

Third, we will answer the question of what the "real" density distribution function looks like, for those state points that cannot be solved with the integral equation, with our simulation result. We must emphasize that all the radial density distributions are obtained under the condition that no phase separation takes place. Figures 3–6 plot the radial density distributions obtained from the current simulation method at various densities under different temperatures. In each plot, there is a one unit shift upward of the functions in order to make the plot clear. The densities we used in our simulation vary from slightly saturated to highly saturated, even for some densities near the spinodal density [17]. For

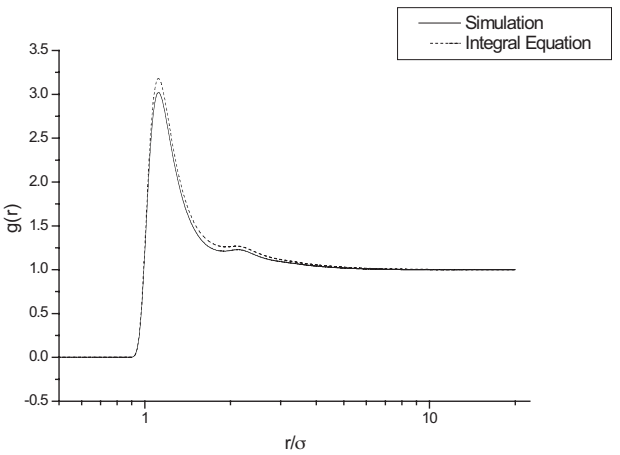

FIG. 2. Radial density distribution functions obtained from the simulation method for $\rho\sigma^3=0.08$ at $T^*=1.0$.

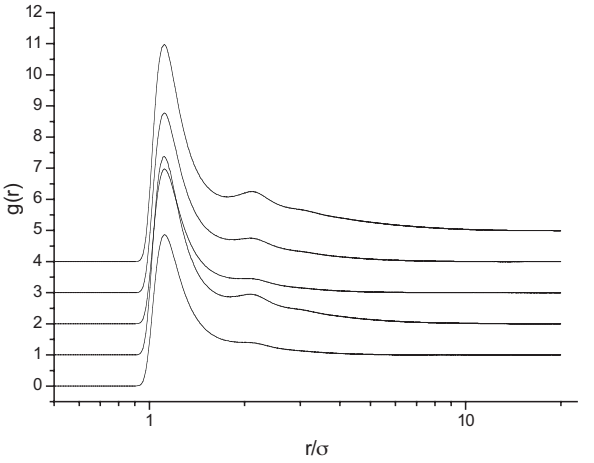

FIG. 3. Radial density distribution functions obtained from the simulation method for $\rho\sigma^3=0.03$, 0.035, 0.04, 0.045, and 0.05 at $T^*=0.75$ and a one unit shift upward is added to the functions in order to make the plot clear.

each temperature, as the density of the system changes from slightly saturated to highly saturated, the structure of the radial density distribution function changes in an interesting way. The second peak of the radial density distribution function first appears, then develops, and finally tends to disappear. The trend is clearly shown in Figs. 4–6; for Fig. 3, where $T^*=0.7$, the second peak first disappears and then develops again. So far it is not very clear what causes the abnormality, and we suspect at low temperature that the mechanism of cluster formation is different from those of high temperature and the phenomenon remains to be explored in the future. This trend is reasonable because as the density approaches the spinodal density, the free-energy barrier to form condensation nuclei goes to zero and even a small density fluctuation can cause homogeneous condensation. Thus, the structure of the system must become more "simple" in order to maintain the one phase state. With all the radial density distribution functions obtained, we do not

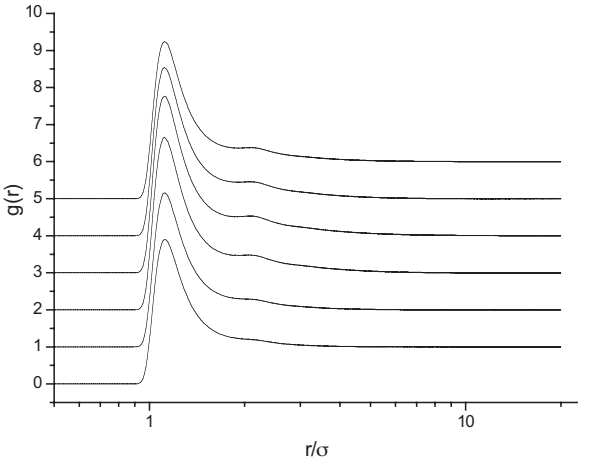

FIG. 4. Radial density distribution functions obtained from the simulation method for $\rho\sigma^3=0.03$, 0.035, 0.04, 0.045, 0.05, and 0.055 at $T^*=0.8$ and a one unit shift upward is added to the functions in order to make the plot clear.

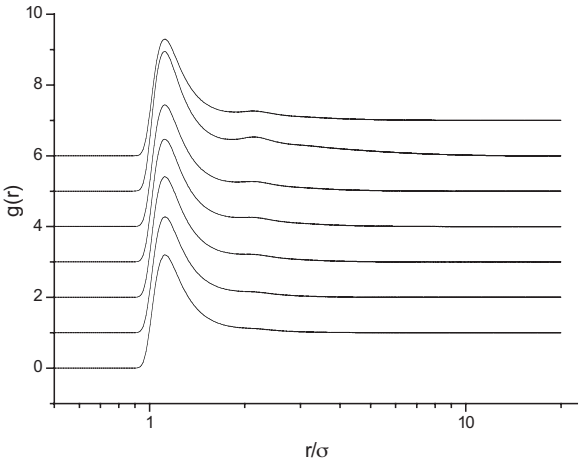

FIG. 5. Radial density distribution functions obtained from the simulation method for $\rho\sigma^3=0.03$, 0.04, 0.05, 0.06, 0.07, 0.08, and 0.085 at $T^*=0.9$ and a one unit shift upward is added to the functions in order to make the plot clear.

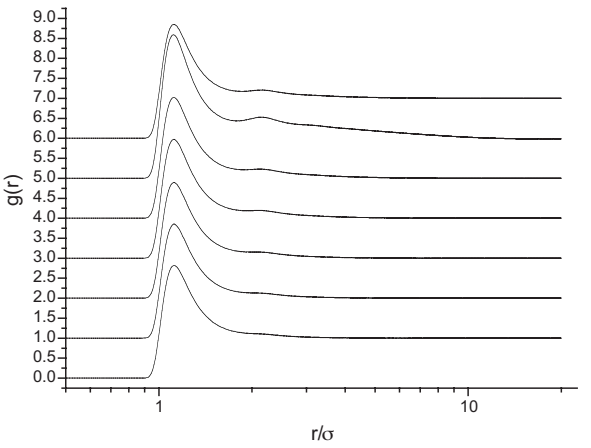

FIG. 6. Radial density distribution functions obtained from both simulation methods for $\rho\sigma^3=0.04$, 0.05, 0.06, 0.07, 0.08, 0.09, and 0.1 at $T^*=1.0$ and a one unit shift upward is added to the functions in order to make the plot clear.

find obvious long-range density fluctuations; here we mean "no obvious" instead of "none" at all. Our findings seem contradictory to some predictions that there should exist obvious long-range density fluctuations as the density approaches the spinodal density [19,20].

IV. SUMMARY

In this work, we extend our simulation of radial density distribution functions of the supersaturated LJ vapor from $T^*=0.7$ to 1.0. Our method provides an effective way to identify the configurations that belong to the phase separation or close to the equilibrium of the metastable state and to compute the radial density distribution function at this interesting material state. From the current simulation result, we find that the widely used integral equation theory cannot accurately predict the thermal properties of metastable systems because the partition function used in that theory does not take into account the density fluctuation of the atoms or molecules. Also, our results indicate that no obvious long-range density fluctuation exists for the real metastable system when the density of the system approaches the spinodal density. In all, we hope that the current work may shed some light on the improvement of the integral equation theory to model the thermal properties of the metastable system.

[1] P. R. Wolde and D. Frenkel, J. Chem. Phys. **109**, 9901 (1998).
[2] D. W. Oxtoby and R. Evans, J. Chem. Phys. **89**, 7521 (1988).
[3] X. C. Zeng and D. W. Oxtoby, J. Chem. Phys. **94**, 4472 (1991).
[4] R. M. Nyquist, V. Talanquer, and D. W. Oxtoby, J. Chem. Phys. **103**, 1175 (1995).
[5] V. Talanquer and D. W. Oxtoby, J. Chem. Phys. **112**, 851 (1999).
[6] B. Senger, P. Schaaf, D. S. Corti, R. Bowles, J. C. Vogel, and H. Reiss, J. Chem. Phys. **110**, 6421 (1999).
[7] K. J. Oh and X. C. Zeng, J. Chem. Phys. **110**, 4471 (1999).
[8] K. J. Oh and X. C. Zeng, J. Chem. Phys. **112**, 294 (2000).
[9] Z. Kozisek, K. Sato, P. Demo, and A. M. Sveshnikov, J. Chem. Phys. **120**, 6660 (2004).
[10] D. I. Zhukhovitskii, J. Chem. Phys. **103**, 9401 (1995).
[11] T. Kraska, J. Chem. Phys. **124**, 054507 (2006).
[12] D. W. Oxtoby, J. Phys.: Condens. Matter **4**, 7627 (1992).
[13] E. Ruckenstein and Y. S. Djikaev, Adv. Colloid Interface Sci. **118**, 51 (2005).
[14] V. G. Baidakov and S. P. Protesenko, High Temp. **41**, 195 (2003).
[15] G. Sh. Boltachev and V. G. Baidakov, High Temp. **41**, 270 (2003).
[16] D. S. Corti and P. Debenedetti, Chem. Eng. Sci. **49**, 2717 (1994).
[17] A. Linhart, C. C. Chen, J. Vrabec, and H. Hasse, J. Chem. Phys. **122**, 144506 (2005).
[18] C. Nie, J. Geng, and W. H. Marlow, J. Chem. Phys. **127**, 154505 (2007).
[19] G. Sarkisov and E. Lomba, J. Chem. Phys. **122**, 214504 (2005).
[20] A. T. Peplow, R. E. Beardmore, and F. Bresme, Phys. Rev. E **74**, 046705 (2006).
[21] L. Benolli, J. Chem. Phys. **98**, 8080 (1993).
[22] R. O. Watts, J. Chem. Phys. **50**, 1358 (1969).
[23] E. Lomba and J. L. Lopez-Martin, J. Stat. Phys. **80**, 825 (1995).
[24] F. Lado, Phys. Rev. **135**, A1013 (1964).
[25] R. Evans, Adv. Phys. **28**, 143 (1979).
[26] J. E. Mayer and E. Montroll, J. Chem. Phys. **9**, 2 (1941).
[27] D. S. Corti, P. G. Debenedetti, S. Sastry, and F. H. Stillinger, Phys. Rev. E **55**, 5522 (1997).
[28] B. Widom, J. Chem. Phys. **39**, 2808 (1963).
[29] M. P. Allen and D. J. Tildesley, *Computer Simulation of Liquids* (Oxford University Press, Oxford, 1989).
[30] D. Frenkel and B. Smit, *Understanding Molecular Simulation* (Academic, New York, 1996).
[31] M. J. Gillan, Mol. Phys. **38**, 1781 (1979).